CFD ANALYSIS OF HYDRODYNAMICS IN A STIRRED MIXING TANK

Dessislava Moutafchieva[1], Hristo Nedelchev[1], Rositsa Stoykova[2], Diyan Tochev[1]

[1]University of Chemical Technology and Metallurgy
8 Kliment Ohridski Blvd., Sofia 1797
Bulgaria, dmoutaf@uctm.edu (D.M.); tochev@uctm.edu (D.T.).
[2]Independent Researcher, Deisenhofen, 82041
Germany, r.stoykova.91@gmail.com (R.S.).
Received 30 June 2026
Accepted 25 August 2026
DOI: 10.59957/jctm.v61.i6.2026.15

ABSTRACT

Design and optimization of mixing tanks require the simultaneous consideration of multiple interdependent parameters, making experimental evaluation both costly and time-consuming. Computational Fluid Dynamics (CFD) provides a powerful alternative for predicting flow behaviour and guiding design decisions. In this study, ANSYS Fluent was employed to investigate the hydrodynamics of a laboratory-scale stirred tank equipped with different impeller geometries. Two modelling approaches were implemented: the Moving Reference Frame (MRF) and the Sliding Mesh (SM) methods. Turbulence was described using the k-ω SST model, and in selected cases, a multiphase analysis was performed using the Volume of Fluid (VOF) approach. Four impellers - two straight-blade impellers with different height-to-diameter ratios, one 45° pitched-blade impeller, and a six-blade Rushton turbine - were evaluated under various operating conditions. The influence of impeller geometry, clearance, and the presence of baffles on the flow field was examined. Experimental visualization was performed to validate the numerical results. The simulations showed good agreement with experimental observations, confirming the reliability of CFD as a predictive and cost-effective tool for mixer design and performance assessment.

Keywords: *computational fluid dynamics, stirred tank, impeller geometry, moving reference frame, volume of fluid, turbulence modelling, flow visualization.*

INTRODUCTION

Mixing tanks are widely used in process industries such as chemical, food, pharmaceutical, biochemical, metallurgical, petroleum processing as well as many others. Multiphase systems, particularly two-phase and three-phase systems, are of major importance in these applications [1, 2]. Mixing is one of the most important unit operations, strongly influencing the quality of the final product. Insufficient mixing can result in non-uniform products, the need for additional downstream separation, and increased waste management costs [3, 4].

The design of stirred tank reactors (STR) depends on the application and is influenced by factors such as tank geometry, impeller type, impeller size and clearance, and the intended process (e.g., blending of miscible liquids, solid suspension, or gas dispersion) [5 - 7]. The power required to rotate the impeller can represent a significant portion of the operating costs, even for vessels of only few cubic meters in volume [8, 9]. Therefore, understanding the hydrodynamics inside STRs is essential for achieving the required mixing performance in an economically optimal manner [10]. Rotating impellers generate highly turbulent, three-dimensional flows through interaction with baffles mounted on the tank wall. These flows are inherently complex and unsteady, making experimental characterization challenging [11 - 13]. Low-Reynolds-number flows often remain non-homogenous and imperfectly mixed [5]. While experimental investigations have provided valuable insights into impeller performance and mixing behaviour, they are limited by factors such as vessel size, equipment complexity, high material costs, measurement accuracy,

and safety considerations [14].

Computational Fluid Dynamics (CFD) has emerged as an effective tool to overcome these limitations. CFD provides detailed information on flow fields, enabling researchers to investigate hydrodynamics, power consumption, mixing time, and other performance indicators under diverse conditions [5, 13 - 16]. Compared to experimental methods, CFD offers advantages such as lower cost, shorter time requirements, greater flexibility, and enhanced repeatability. Commercial CFD packages, such as ANSYS Fluent, have become widely adopted for simulating and analysing stirred tanks and provide detailed predictions necessary for equipment design and optimization [17 - 19].

Accurate CFD modelling of stirred tanks requires careful selection of the computational grid, discretization scheme, impeller rotation model, and turbulence model [20, 21]. Impeller rotation is often modelled using the Moving Reference Frame (MRF) approach, in which the computational domain is divided into stationary and rotating zones. By solving the governing equations in a rotating frame of reference, the inherently unsteady flow induced by the impeller can be approximated as steady state [21, 22]. The velocity transformation is expressed as Eq. (1) and Eq. (2).

$$\vec{v}_r = \vec{v} - \vec{u}_r \quad (1)$$

$$\vec{u}_r = \vec{v}_t + \vec{\omega} \times \vec{r} \quad (2)$$

where $\vec{v}_r$ is the relative velocity, $\vec{v}$ the absolute velocity, $\vec{u}_r$ the velocity of the moving frame relative to the inertial reference frame, $\vec{v}_t$ the translational frame velocity, and $\vec{\omega}$ the angular velocity.

Alternative approaches include the sliding mesh method, which explicitly resolves impeller motion in time, and the Volume of Fluid (VOF) method, which is used to capture phase interfaces in partially filled vessels. In the VOF method, the volume fraction α_q of phase q is tracked in each computational cell, where $\alpha_q = 0$ indicates absence of the phase, $\alpha_q = 1$ indicates full presence, and $0 < \alpha_q < 1$ denotes an interface [20, 23].

Turbulence modelling presents a particular challenge for stirred tank simulations. Direct Numerical Simulation (DNS) and Large Eddy Simulation (LES) provide high-fidelity results but are computationally prohibitive for the high Reynolds numbers (typically >50,000) encountered in industrial applications [10, 23, 24]. Consequently, these approaches are rarely applied for practical impeller design. Instead, most studies rely on Reynolds-Averaged Navier-Stokes (RANS) models. Among these, the realizable k-ε and the k-ω SST models are widely used due to their ability to account for shear stress transport and predict eddy viscosity. Previous studies have shown that MRF combined with RANS models provides reliable results for stirred tank flows [25, 26].

The objective of the present work is to perform a systematic CFD analysis of a laboratory-scale stirred tank using ANSYS Fluent. The study focuses on evaluating the influence of impeller geometry, impeller clearance, and baffle configuration on the resulting flow field. In addition, experimental flow visualization techniques are employed to provide qualitative validation of the predicted hydrodynamic behaviour.

Although CFD modelling of stirred tanks has been extensively investigated, the combined influence of impeller geometry, clearance, and the size of the rotating computational domain has received comparatively less attention in laboratory-scale systems. In this work, CFD simulations based on the MRF approach and the realizable k-ε turbulence model are used to investigate these effects and to compare the predicted circulation patterns with experimental observations.

EXPERIMENTAL

Experimental setup

A cylindrical stirred tank reactor with and without baffles was designed and fabricated from polymethylmethacrylate (PMMA), selected for its transparency and glass-like optical properties. The tank had an outer diameter of 200 mm, a height of 290 mm, and a wall thickness of 3 mm. The baffles were four, with a thickness of 3 mm, their width was 1/10th of the tank's diameter (20 mm) and the distance to the bottom is the same as that of the impeller (26 mm). An impeller was positioned 26 mm above the bottom of the reactor. Four impeller geometries were designed in SolidWorks 2017 and subsequently 3D-printed using polylactic acid (PLA) filament. These included two straight-blade impellers with height-to-diameter ratios of 32.5/65 mm and 21.67/65 mm, one pitched-blade impeller with blades inclined at 45°, and one six-blade Rushton turbine. This equipment was selected as it represents

a standard stirred-tank design while being sufficiently compact to permit computational investigation with a fine mesh resolution.

CFD setup

A 3D CAD model of the stirred tank reactor was created in ANSYS SpaceClaim. The computational domain included the tank geometry and a single impeller configuration (Fig. 1).

The geometry was discretized using the Finite Volume Method (FVM). A poly-hexcore mesh, consisting of 512 000 elements, also referred to as "mosaic" meshing, was employed to achieve a balance between computational efficiency and accuracy. Representative discretization of the domain is presented in Fig. 2.

The governing equations solved in the simulations include the continuity equation, representing mass conservation Eq. (3), and the Navier-Stokes equation, representing momentum conservation Eq. (4).

Continuity Eq. (3) is as follow:

$$\frac{\partial \rho}{\partial t} + \nabla \rho \vec{v}_T = 0 \tag{3}$$

Navier-Stokes Eq. (4) is as follow:

$$\frac{\partial}{\partial t}\rho\vec{v} + \nabla \cdot (\rho\vec{v}_r\vec{v}) + \rho[\vec{\omega} \times (\vec{v} - \vec{v}_t)] = -\nabla p + \nabla \cdot \bar{\tau} + \vec{F} \tag{4}$$

where ρ is fluid density, $\vec{v}$ is absolute velocity, $\vec{v}_r$ is relative velocity, $\vec{v}_t$ is translational velocity, $\vec{\omega}$ is angular velocity, p is pressure, $\bar{\tau}$ is stress tensor, $\vec{F}$ is external source term.

These equations form the basis of the CFD model implemented in ANSYS Fluent and were solved to obtain the velocity and pressure distributions within the stirred tank.

The simulations were conducted under steady-state conditions. The turbulence was modelled using the realizable k-ε model, selected for its proven accuracy in stirred tank simulations. Water at 25°C was chosen as the working fluid from the Fluent materials database.

The top surface of the vessel was modelled as a wall with zero shear stress in all directions to approximate a free-surface behaviour. The revolutions in the rotational area and on the shaft are identical. The rotation of the impeller was modelled with the MRF (Moving Reference Frame) approach, in which mass (Eq. (3)) and momentum conservation (Eq. (4)) equations are solved to determine the flow variables such as velocity and pressure.

Pressure-velocity coupling was achieved using the SIMPLE algorithm. To accelerate convergence, Full Multi Grid (FMG) initialization, which solves simplified governing equations on a coarser mesh, was applied in addition to the standard initialization procedure.

RESULTS AND DISCUSSION

Essential aspect of mixing equipment design is to avoid "dead" zones. They are regions of low velocity where mixing is minimal or non-existent, causing reduced effective volume and altered residence times.

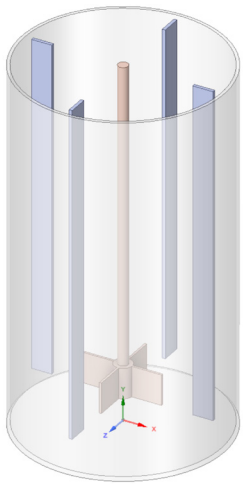


Fig. 1. 3D CAD model of mixing tank with baffles and straight blade impeller.

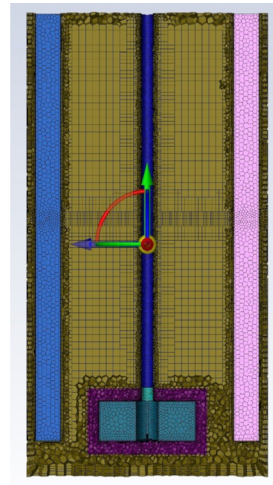


Fig. 2. Computational mesh of stirred tank reactor equipped with four baffles.

Therefore, velocity distribution was selected as one of the key parameters monitored in this study. Four impellers were examined: two straight-blade impellers with different height-to-diameter ratios (32.5/65 mm and 21.67/65 mm), one pitched-blade impeller with blades inclined at 45°, and one six-blade Rushton turbine (Fig. 3).

Influence of impeller geometry

Five simulations were performed with each of the two straight-blade impellers. The impeller speed was varied systematically (170, 200, 230, 260, and 290 rpm), while all other conditions were kept constant.

The flow patterns were analysed using contour plots on a central vertical plane and three-dimensional iso-volumes representing regions with a velocity magnitude greater than 0.33 m s^{-1}. These visualization techniques showed distinct circulation zones associated with each impeller geometry. Increasing the impeller speed from 170 to 290 rpm resulted in a progressive rise in both tangential and axial velocity components. The maximum velocity values occurred near the blade tips and along the flow jet directed towards the tank walls (Fig. 4a).

Fig. 4b compares the high-velocity regions for

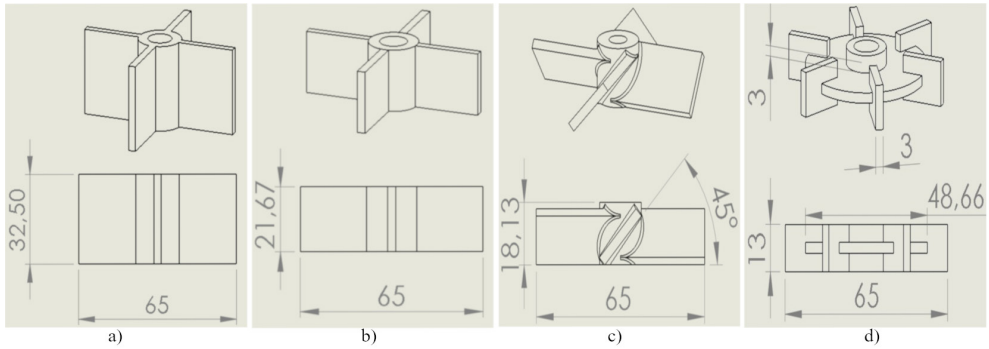


Fig. 3. Geometry of the used impellers: (a) straight-blade impeller with h/d = 0.50, (b) straight-blade impeller with h/d = 0.33, (c) pitched-blade impeller (45°), and (d) six-blade Rushton turbine

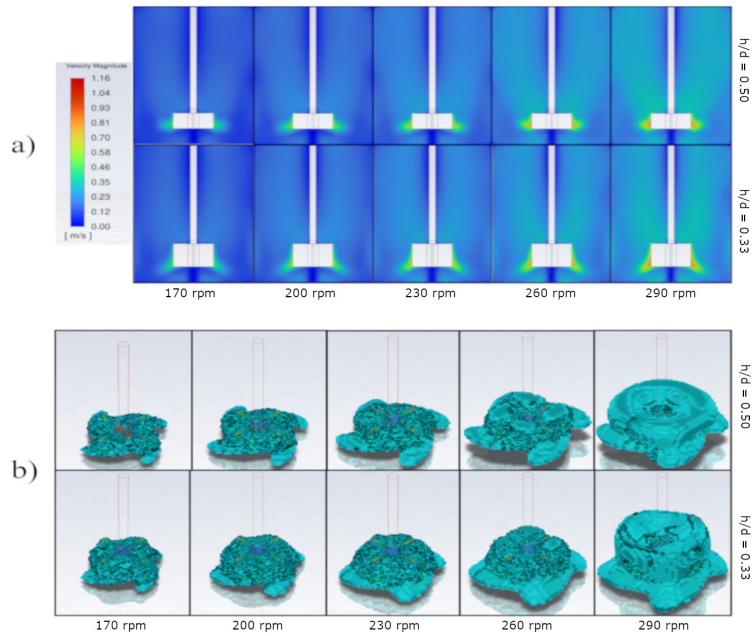


Fig. 4. Effect of impeller geometry and rotational speed on the flow field generated by straight-blade impellers: (a) velocity magnitude contours of the two straight blade impellers obtained using the MRF method and (b) iso-volume visualization of regions where the velocity magnitude exceeds 0.33 m s^{-1}.

the two straight-blade impellers. The taller impeller (h/d = 0.50) generated a more pronounced axial flow and reduced low-velocity regions at the tank bottom, while the shorter impeller (h/d = 0.33) exhibited stronger radial flow but weaker top-to-bottom circulation.

The maximum velocity in the mixing volume increased almost linearly with rotational speed (Fig. 5), supporting the expected proportionality between tip speed and impeller rotation rate.

Influence of impeller clearance from the tank bottom

Another set of five simulations were conducted using the pitched-blade impeller (45°) to investigate the influence of impeller clearance (distance from the tank bottom) on the flow structure. Clearances (C) of 22, 26, 30, 34, and 38 mm were investigated at a constant rotation speed of 200 rpm.

The results indicated that the clearance strongly affects both the magnitude and uniformity of the velocity field (Fig. 6a). The optimal clearance was found to be approximately 26 mm, at which the maximum average velocity (0.82 m s^{-1}) and minimal stagnation zones were observed. Smaller clearances led to increased wall shear but restricted flow recirculation above the impeller, while larger clearances reduced fluid exchange between the upper and lower zones of the tank.

Velocity profiles plotted along a vertical line 17.5 mm from the impeller axis (Fig. 7b) confirmed the sensitivity of the axial flow distribution to clearance

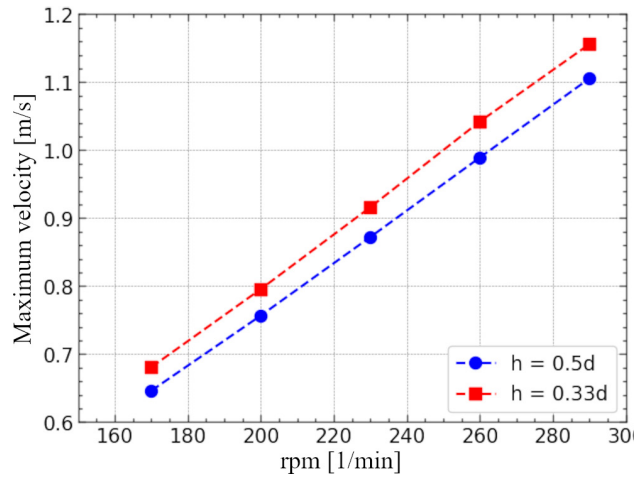


Fig. 5. Comparison of maximum velocities in the tank at different impeller speeds, where h denotes blade height and d the impeller diameter.

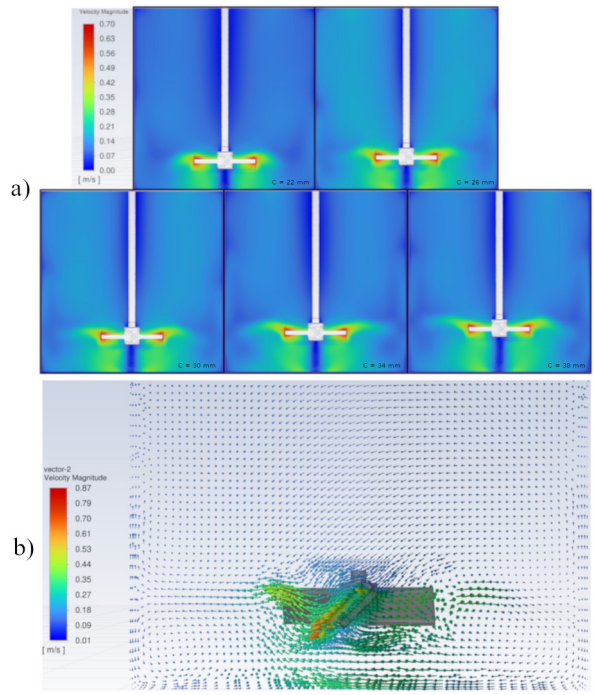


Fig. 6. Effect of impeller clearance from the tank bottom on the velocity field at an impeller speed of 200 rpm: (a) velocity magnitude contours in the central vertical plane for different impeller clearances and (b) velocity vector field illustrating the flow direction and magnitude around the impeller region.

height, particularly near the tank bottom.

Path line analysis showed a well-defined downward axial jet and an upward return flow near the tank walls, in agreement with experimental visualization (Fig. 7).

Influence of rotational domain size

To evaluate the sensitivity of the numerical solution to the size of the rotational domain, six configurations of the Rushton turbine were simulated (Table 1). The height (H) and diameter (D) of the rotating region were varied systematically while maintaining the same impeller geometry and operating conditions.

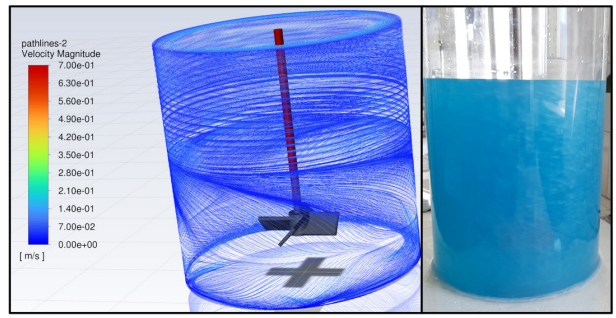
The velocity contours (Fig. 8) revealed that an excessively small rotational zone (e.g., δ = 0.5 mm) caused artificial velocity gradients near the interface between rotating and stationary regions, due to insufficient overlap for flux continuity. Conversely, an excessively large zone (δ = 15 mm) increased computational cost without improving solution accuracy. The optimal configuration was achieved for H = 28 mm, D = 80 mm and δ = 7.5 mm, which provided stable velocity predictions and minimal numerical diffusion.

Influence of baffles on flow structure

The presence of baffles significantly influences the hydrodynamic behaviour in stirred tank reactors. Fig. 9 the flow field obtained from the CFD simulations

Table 1. Parametric configurations of the rotating (MRF) domain surrounding the impeller: height H, diameter D, and wall clearance δ.

No	H, mm	D, mm	δ, mm
1	23	75	5
2	28	80	7.5
3	33	85	10
4	38	90	12.5
5	43	95	15
6	14	66	0.5



a) b)

Fig. 7. Flow behaviour near the vessel wall: (a) simulation result and (b) experimental observation.

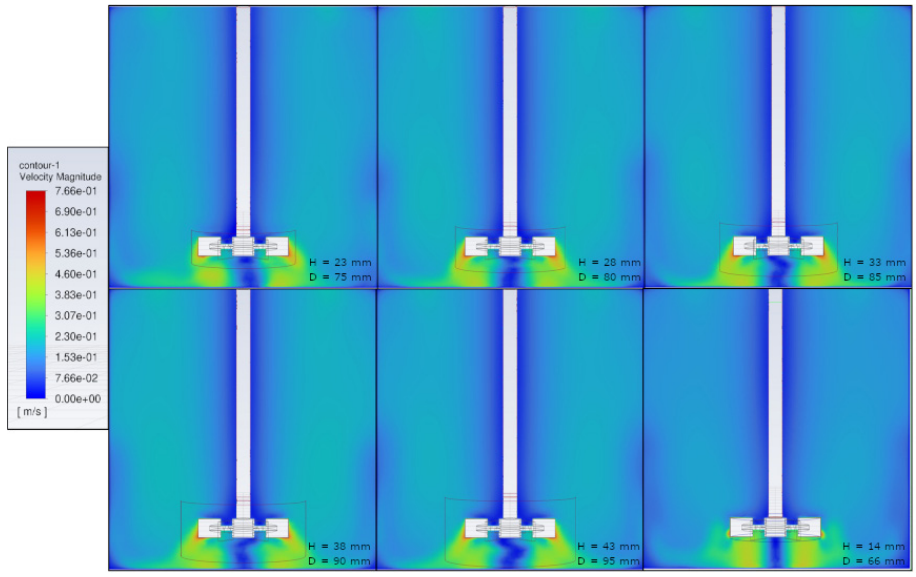


Fig. 8. Velocity contours showing the effect of the rotational domain size at 200 rpm.

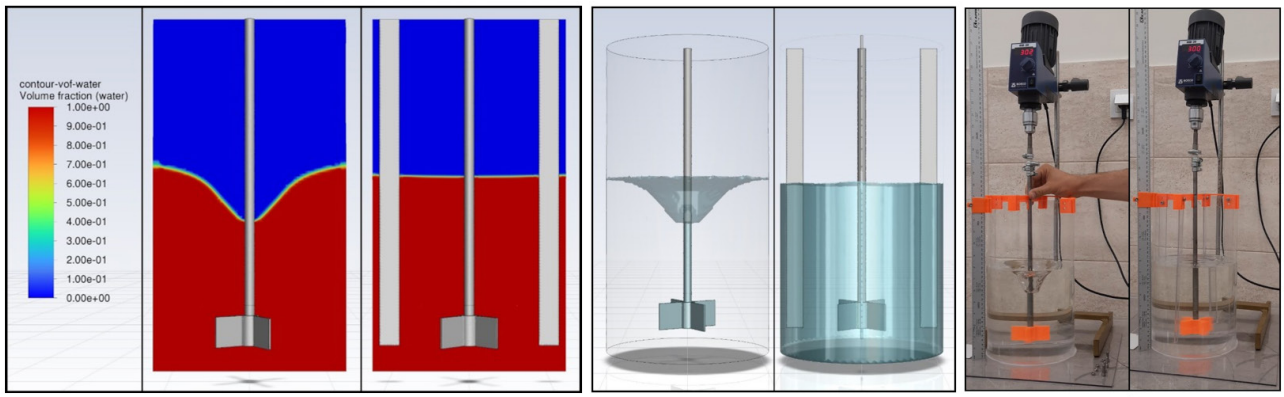


Fig. 9. Influence of baffles on the flow structure in the stirred tank reactor: (a) contour of water's volume fraction: left - unbaffled tank with vortex formation; right - baffled tank where vortex formation is suppressed, (b) comparison of the flow characteristics of unbaffled and baffled configurations, and (c) experimental setup used for flow visualization and validation of the CFD results: left - reactor without baffles showing vortex formation; right - reactor equipped with four equally spaced vertical baffles.

and experimental visualization, comparing the mixing conditions with and without baffles.

In the absence of baffles, the rotating impeller generates a strong tangential flow component that induces a pronounced swirling motion within the vessel. As a result, a central vortex forms at the liquid surface. This vortex formation is undesirable because it reduces mixing efficiency, promotes air entrainment, and limits axial circulation within the tank.

The CFD simulations also reveal the presence of low-velocity regions and zones of weak recirculation in the unbaffled configuration. These "dead zones" correspond to areas where fluid motion is minimal, leading to poor mixing and longer homogenization times.

When four equally spaced vertical baffles are introduced along the tank wall, the flow structure changes substantially. The baffles disrupt the rotational motion of the fluid and convert tangential velocity into radial and axial components. Consequently, vortex formation is suppressed, and stronger circulation loops develop between the impeller region and the upper part of the vessel.

The resulting flow field becomes more uniform, and turbulence intensity increases near the tank walls and around the impeller blades. These effects enhance overall mixing efficiency and reduce stagnant regions within the vessel.

The CFD predictions (Fig. 9a and Fig. 9b) are consistent with the experimental flow visualization shown in Fig. 9c, where the unbaffled configuration exhibits a clear vortex and swirling motion, while the baffled configuration demonstrates improved circulation and more homogeneous mixing throughout the tank.

Experimental validation of CFD results

To validate the numerical predictions, three complementary visualization methods were employed: (i) dispersion of solid insoluble particles, (ii) addition of a food-grade dye, and (iii) illumination of a rheoscopic fluid containing reflective silicate platelets. Each method provided distinctive insights into flow behaviour.

The motion of solid particles (Fig. 8a) revealed the initial formation of circulation loops, while the dye visualization (Fig. 8b) highlighted mixing time and homogenization rate. The rheoscopic fluid offered the clearest representation of vortical structures and velocity gradients under dynamic illumination (Fig. 8c).

The experimentally observed flow patterns were in good qualitative agreement with the CFD predictions. In particular, the presence of strong swirling motion in the unbaffled configuration and the more uniform circulation pattern in the baffled tank were consistently observed in both the experiments and the simulations. This agreement indicates that the MRF approach combined with the realizable k-ε turbulence model provides a reliable representation of the steady-state hydrodynamics within the stirred tank.

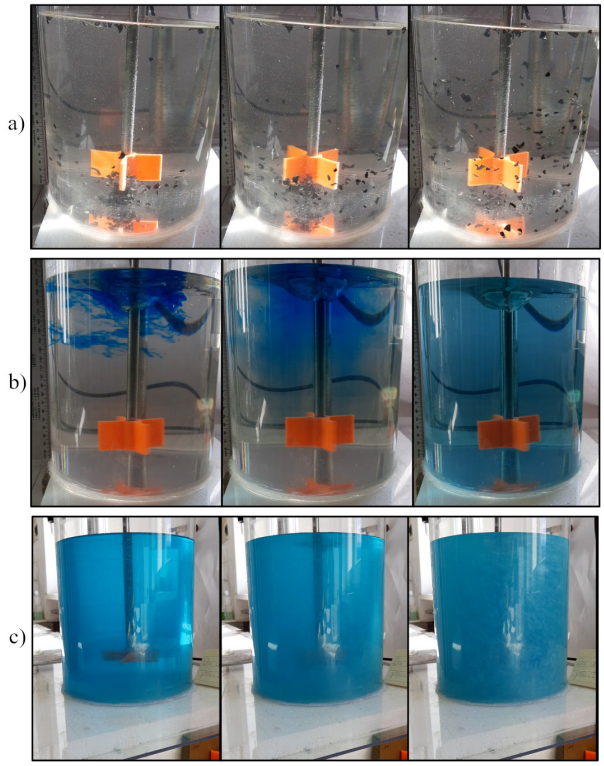


Fig. 10. Experimental flow visualization methods used for validation: (a) distribution of solid particles indicating flow circulation within the tank; (b) mixing process visualized by the dispersion of a food-grade dye; (c) flow patterns revealed using a rheoscopic fluid.

CONCLUSIONS

The combined CFD and experimental study provides the following key insights:

- Impeller Geometry: The blade height-to-diameter ratio affects axial circulation and the extent of "dead" zones; higher blades promote stronger vertical mixing.
- Impeller Clearance: Optimal clearance (≈26 mm) ensures balanced flow distribution and prevents stagnation near the tank bottom.
- Rotational Domain Size: Appropriate domain dimensions are crucial for numerical stability and accuracy; excessive size increases computational cost without improving fidelity.
- Baffles: The presence of baffles eliminates central vortex formation, improving mixing efficiency and reducing free-surface deformation.
- Model Validation: Strong qualitative agreement between CFD and experimental visualizations validates the selected turbulence and impeller rotation models.

Overall, the results confirm that CFD simulations, when properly configured and validated, can serve as a powerful and cost-effective tool for optimizing stirred tank designs and predicting mixing performance.

Acknowledgments

This study was funded by the European Union-NextGenerationEU, through the National Recovery and Resilience Plan of the Republic of Bulgaria, project № BG-RRP-2.004-0002, "BiOrgaMCT".

Authors' contributions

D.M.: conceptualization, methodology, investigation, writing - original draft, funding acquisition, project administration; H.N.: methodology, investigation, visualization; R.S.: conceptualization, methodology, writing - original draft, review & editing; D.T.: review & editing, funding acquisition, project administration.

REFERENCES

1. E.L. Paul, V.A. Atiemo-Obeng, S.M. Kresta, Hoboken, Handbook of Industrial Mixing: Science and Practice, John Wiley & Sons Inc., 2004.
2. M. Ge, J. Chen, L. Zhao, G. Zheng, Mixing Transport Mechanism of Three-Phase Particle Flow Based on CFD-DEM Coupling, Processes, 11, 6, 2023, 1619-1636.
3. P. Cullen, S. Bakalis, C. Sullivan, Advances in control of food mixing operations, Current Opinion in Food Science, 17, 2017, 89-93.
4. R.P. Utikar, V.V. Ranade, Intensifying Multiphase Reactions and Reactors: Strategies and Examples, ACS Sustainable Chemistry & Engineering, 5, 5, 2017, 3607-3622.
5. A. Salho, D. Hamzeh, A Review of Stirred Tank Dynamics: Power Consumption, Mixing Time and Impeller Geometry, International Journal of Heat and Technology, 42, 3, 2024, 1081-1092.
6. L. Böhm, L. Hohl, C. Bliatsiou, M. Kraume, Multiphase Stirred Tank Bioreactors - New Geometrical Concepts and Scale-up Approaches, Chemie Ingenieur Technik, 91, 12, 2019, 1724-1746.
7. A. Reid, R. Rossi, C. Cottini, A. Benassi, CFD simulation of a Rushton turbine stirred-tank using open-source software with critical evaluation of MRF-based rotation modeling, Meccanica, 60, 2025, 1613-1637.
8. H. Ameur, Energy efficiency of different impellers in stirred tank reactors, Energy, 93, 2, 2015, 1980-1988.
9. G. Ascanio, B. Castro, E. Galindo, Measurement of Power Consumption in Stirred Vessels-A Review, Chemical Engineering Research and Design, 82, 9, 2004, 1282-1290.
10. J.B. Joshi, N.K. Nere, C.V. Rane, B.N. Murthy, C.S. Mathpati, A.W. Patwardhan, V.V. Ranade, CFD simulation of stirred tanks: Comparison of turbulence models. Part I: Radial flow impellers. Can. J. Chem. Eng., 89, 1, 2011, 23-82.
11. J. Gimbun, C.D. Rielly, Z.K. Nagy, J.J. Derksen, Detached eddy simulation on the turbulent flow in a stirred tank. AIChE J., 58, 10, 2012, 3224-3241.
12. C. Mayorga, J. Morchain, A. Liné, Reconstruction of the 3D hydrodynamics in a baffled stirred tank using Proper Orthogonal Decomposition, Chemical Engineering Science, 248, A, 2022, 117220.
13. X. Hu, A. Ilgun, A. Passalacqua, R. Fox, F. Bertola, M. Milosevic, F. Visscher, CFD simulations of stirred-tank reactors for gas-liquid and gas-liquid-solid systems using OpenFOAM®, International Journal of Chemical Reactor Engineering, 19, 2, 2021, 193-207.
14. M. Jaszczur, A. Młynarczykowska, A general review of the current development of mechanically agitated vessels, Processes, 8, 8, 2020, 982.
15. A. Ochieng, M.S. Onyango, CFD Simulation of Solids Suspension in Stirred Tanks: Review, Hem. ind., 64, 5, 2010, 365-374.
16. K. Youcef, Z. Driss, M. Foukrach, S. Rosa, T. Baki, A CFD investigation of the performance of stirred tanks, J. Serb. Chem. Soc., 90, 11, 2025, 1369-1382.
17. G. Mittal, R.I. Kikugawa, Computational fluid dynamics simulation of a stirred tank reactor, Materials Today: Proceedings, 46, 20, 2021, 11015-11019.
18. A. Panunzi, M. Moroni, A. Mazzelli, M. Bravi, Industrial Case-Study-Based Computational Fluid Dynamic (CFD) Modeling of Stirred and Aerated Bioreactors, ACS Omega, 7, 29, 2022, 25152-25163.
19. R. Stoykova, D. Moutafchieva, D. Popova, V. Iliev, Gas hold-up prediction in gas-liquid stirred tank reactor using CFD simulation, J. Chem. Technol. Metall, 49, 5, 2014, 469-472.
20. D.A. Deglon, C.J. Meyer, CFD Modelling of Stirred Tanks: Numerical Considerations. Minerals Engineering, 19, 2006, 1059-1068.
21. ANSYS Inc., ANSYS Fluent Theory Guide, 2023.
22. H. Patil, A.K. Patel, H.J. Pant, A. Venu Vinod, CFD simulation model for mixing tank using multiple reference frame (MRF) impeller rotation, ISH Journal of Hydraulic Engineering, 27, 2, 2021, 200-209.
23. F.L. Yang, S.J. Zhou, Free Surface Turbulent Flow in an Unbaffled Stirred Tank: Detached Eddy Simulation and VOF Study, Chem. Biochem. Eng. Q., 29, 3, 2015, 395-403.
24. S.L. Yeoh, G. Papadakis, M. Yianneskis, Numerical Simulation of Turbulent Flow Characteristics in a Stirred Vessel Using the LES and RANS Approaches with the Sliding/Deforming Mesh Methodology, Chemical Engineering Research and

Design, 82, 7, 2004, 834-848.
25. R. Zadghaffari, J.S. Moghaddas, J. Revstedt, A mixing study in a double-Rushton stirred tank, Computers & Chemical Engineering, 33, 7, 2009, 1240-1246.
26. M. Coroneo, G. Montante, A. Paglianti, F. Magelli, CFD prediction of fluid flow and mixing in stirred tanks: Numerical issues about the RANS simulations, Computers and Chemical Engineering, 35, 10, 2011, 1959-1968.